

- [3] E. Boch, "Backhaul for WiMax and LTE: High bandwidth ethernet radio systems," *Microw. J.*, pp. 22–26, Nov. 2008.
- [4] P. Hallbjorn, "The significance of radiation efficiencies when using S-parameters to calculate the received signal correlation from two antennas," *IEEE Antennas Wireless Propag. Lett.*, vol. 4, pp. 97–99, 2005.
- [5] K. Chung and J. H. Yoon, "Integrated MIMO antenna with high isolation characteristic," *Electron. Lett.*, vol. 43, no. 4, Feb. 2007.
- [6] S. Zhang, J. Xiong, and S. He, "MIMO antenna system of two closely-positioned PIFAs with high isolation," *Electron. Lett.*, vol. 45, no. 15, Jul. 2009.
- [7] H. Li, J. Xiong, and S. He, "A compact planar MIMO antenna system of four elements with similar radiation characteristics and isolation structure," *IEEE Antennas Wireless Propag. Lett.*, vol. 8, pp. 1107–1110, 2009.
- [8] C. H. Lee, S. Y. Chen, and P. Hsu, "Integrated dual planar inverted-F antenna with enhanced isolation," *IEEE Antennas Wireless Propag. Lett.*, vol. 8, pp. 963–965, 2009.
- [9] 3GPP TS 36.101, V8.3.0, EUTRA User Equipment Radio Transmission and Reception 2008.
- [10] C. Y. Chiu *et al.*, "Reduction of mutual coupling between closely-packed antenna elements," *IEEE Trans. Antennas Propag.*, vol. 55, no. 6, pp. 1732–1738, Jun. 2007.
- [11] K. S. Min, D. J. Kim, and Y. M. Moon, "Improved MIMO antenna by mutual coupling suppression between elements," in *Proc. Eur. Conf. on Wireless Technology*, Paris, France, Oct. 2005, pp. 125–128.

Mode-Based Estimation of 3 dB Bandwidth for Near-Field Communication Systems

Youndo Tak, Jongmin Park, and Sangwook Nam

Abstract—A new method for estimating the 3 dB bandwidth of near-field communication (NFC) systems using identical electrically small antennas is proposed. The method is based on equivalent circuit representation using the addition theorem, an approach used in the analysis of coupled antennas, and the correction factor derived from antenna impedance characteristics. In addition, variation in the 3 dB bandwidth with respect to the relative position and orientation of the NFC system is investigated using the proposed method.

Index Terms—Addition theorem, antenna equivalent circuit, bandwidth estimation, capacity, electrically small antenna, near-field communication (NFC), near-field coupling.

I. INTRODUCTION

It is well-known that the space around an antenna can be classified into the far-field region and near-field region. In the near-field region, reactive energy, which is stored and oscillated in space, is dominant [1]. The near field of an antenna possesses greater available power and faster power roll-off than the far field of the antenna, so it is suitable for constructing efficient body area communication systems [2], [3].

The capacity of a communication system is the maximum data rate that can be achieved by the system, and this is strongly related to the 3

Manuscript received August 15, 2010; revised November 18, 2010; accepted January 15, 2011. Date of publication June 09, 2011; date of current version August 03, 2011. This work was supported by the National Research Foundation of Korea (NRF) grant funded by the Korean government (MEST) (No.2010-0018879).

The authors are with the School of Electrical Engineering and INMC, Seoul National University, Seoul 151-742, Korea (e-mail: ydtak76@snu.ac.kr).

Color versions of one or more of the figures in this communication are available online at <http://ieeexplore.ieee.org>.

Digital Object Identifier 10.1109/TAP.2011.2158960

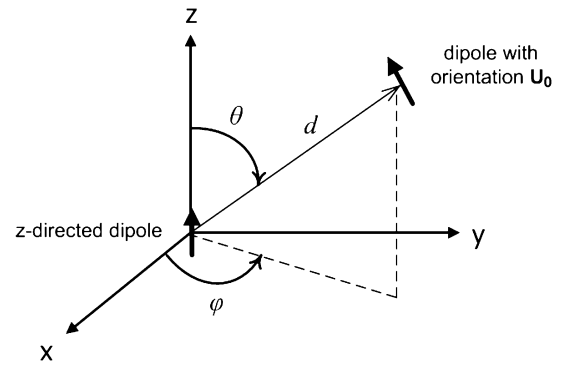


Fig. 1. Two coupled short dipoles with arbitrary orientation [11].

dB bandwidth of the system according to the Shannon-Hartley theorem [4]. Recently, a study on the bandwidth and the capacity of a near-field communication (NFC) system was reported using the equivalent circuit model that is used for conventional RF-ID in [5]. However, this does not consider the intrinsic impedance characteristics of the solenoidal loop antenna. In this communication, we attempt to determine the 3 dB bandwidth of an NFC system using identical antennas that are coupled for transmitting and receiving information.

II. EQUIVALENT CIRCUIT REPRESENTATION OF AN NFC SYSTEM BASED ON THE ADDITION THEOREM

The impedance characteristics of an antenna can be equivalently approximated as an RLC resonator. Therefore, the equivalent circuit of the coupled antennas can be expressed based on the equivalent circuit of the coupled resonator [6]. However, in contrast to conventional coupled resonators, whose coupling network is composed of only imaginary elements, the coupling network of antennas needs to be comprised of a real element as well as imaginary elements due to the different radiation resistances of the even mode and odd mode [7], [8].

When electrically small antennas (ESAs) are coupled to each other in an NFC system, their mutual impedance can be expressed by the mode-based approach using the addition theorem because ESAs predominantly generate a TE_{10} or TM_{10} mode [9], [10]. If two short dipoles that generate TM_{10} modes are coupled to each other, as shown in Fig. 1, the mutual impedance is given as (1), shown at the bottom of the next page, where η is the free space impedance, $\mathbf{U}_0 = x_0 u_1 + y_0 u_2 + z_0 u_3$ is a unit vector representing the orientation of the second antenna, R_r is the radiation resistance of the antenna, kd is the electrical distance between the coupled antennas, and $\dot{H}_1^{(2)}(x)$ is the spherical Hankel function whose derivative is given as $\dot{H}_1^{(2)}(x)$ [11]. In addition, in terms of the small loops (or the magnetic dipoles) that generate the TE_{10} modes, the mutual impedance is the same as in (1) due to the duality of the electric dipole and the magnetic dipole.

As shown in Fig. 2, the equivalent circuit for coupled antennas can be expressed by the conventional T-equivalent circuit of a 2-port network. In the equivalent circuit, the tuned antenna is represented as the series resonant circuit by R_a and L_a , which are the resistance and the reactance of the antenna itself, respectively, with the tuning capacitor C_s . In addition, the mutual inductance, L_{12} , and mutual resistance, R_{12} , can be defined as real and imaginary elements of mutual impedance; this is obtained from (1). The source and the load impedances are given as R_G and R_L .

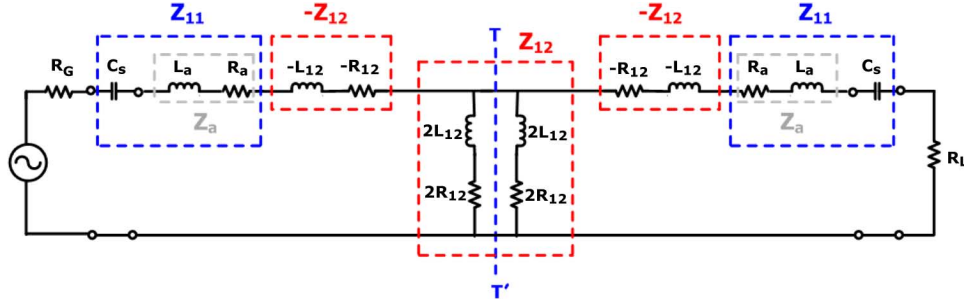


Fig. 2. Proposed equivalent circuit of two coupled small antennas.

III. BANDWIDTH CALCULATION BASED ON THE EQUIVALENT CIRCUIT

According to the conventional network analysis method for symmetrical 2-port networks, the transmission parameter of the coupled network can be expressed using the reflection parameters of the network for odd-mode and even-mode resonances [12]:

$$S_{21} = \frac{1}{2}(S_{11,e} - S_{11,o}) = \frac{1}{2} \left(\frac{Z_{in,e} - R_G}{Z_{in,e} + R_G} - \frac{Z_{in,o} - R_G}{Z_{in,o} + R_G} \right). \quad (2)$$

For the proposed circuit, which is shown in Fig. 2, the input impedance of the coupled antenna for the odd-mode and even-mode can be given as:

$$Z_{in,e}(\omega) = R_a + j\omega_s L_a \left(\frac{2\Delta\omega}{\omega_s} \right) + j\omega L_{12} + R_{12} \quad (3)$$

$$Z_{in,o}(\omega) = R_a + j\omega_s L_a \left(\frac{2\Delta\omega}{\omega_s} \right) - j\omega L_{12} - R_{12} \quad (4)$$

with the resonant frequency of the antenna, given as:

$$\omega_s = (L_a C_s)^{-0.5} \quad (5)$$

and the operating frequency, given by:

$$\omega = \omega_s + \Delta\omega. \quad (6)$$

Therefore, the transmission parameter of the circuit is shown in (7), as the bottom of the page, when additional parameters are defined as

$$Q_e = \frac{\omega_0 L_a}{R_G} = \frac{1}{\omega_0 C_s R_G} \quad (8)$$

and

$$Q_k = \frac{j\omega L_{12}}{R_G}. \quad (9)$$

TABLE I
PARAMETERS FOR PROPOSED CHARACTERISTIC EQUATION

Parameter	Expression
a_4	Q_e^4
a_2	$2Q_e^2 \left\{ \left(\frac{R_a}{R_G} + 1 \right)^2 + \left(\frac{R_{12}}{R_G} \right)^2 - Q_k^2 \right\}$
a_1	$-8Q_k Q_e \left(\frac{R_{12}}{R_G} \right) \left(\frac{R_a}{R_G} + 1 \right)$
a_0	$-\left[\left(\frac{R_a}{R_G} + 1 \right)^4 + \left(\frac{R_{12}}{R_G} \right)^4 + Q_k^4 - 2 \left\{ \left(\frac{R_{12}}{R_G} \right)^2 - Q_k^2 \right\} \left(\frac{R_a}{R_G} + 1 \right)^2 + 2Q_k^2 \left(\frac{R_{12}}{R_G} \right)^2 \right]$

According to (7), the 3 dB fractional bandwidth can be evaluated by characteristic (10) using parameters represented in Table I:

$$a_4 \left(\frac{2\Delta\omega}{\omega_s} \right)^4 + a_2 \left(\frac{2\Delta\omega}{\omega_s} \right)^2 + a_1 \left(\frac{2\Delta\omega}{\omega_s} \right) + a_0 = 0. \quad (10)$$

IV. EXAMPLES

A. Dominant Mode

The method is demonstrated by investigating the 3 dB bandwidth characteristics of 10-turn solenoidal small loop antennas, which are made of copper wire. According to the ratio of the radius to the height of the antenna, the antennas are classified as wide case and narrow case,

$$Z_{12(TM10-TM10)} = \frac{3R_r}{2} \left[\frac{2\hat{H}_1^{(2)}(kd) \cos \theta \{ \cos \varphi \sin \theta u_1 + \sin \varphi \sin \theta u_2 + \cos \theta u_3 \}}{\eta k d^2 \omega \varepsilon} - \frac{\hat{H}_1^{(2)}(kd) \sin \theta \{ \cos \varphi \cos \theta u_1 + \sin \varphi \cos \theta u_2 - \sin \theta u_3 \}}{k d} \right] \quad (1)$$

$$S_{21} = \frac{2 \left(\frac{R_{12}}{R_G} - jQ_k \right)}{\left[\left\{ \left(\frac{R_a}{R_G} + 1 \right)^2 - \left(\frac{R_{12}}{R_G} \right)^2 - Q_e^2 \left(\frac{2\Delta\omega}{\omega_s} \right)^2 + Q_k^2 \right\} + 2j \left\{ Q_e \left(\frac{R_a}{R_G} + 1 \right) \left(\frac{2\Delta\omega}{\omega_s} \right) - Q_k \left(\frac{R_{12}}{R_G} \right) \right\} \right]} \quad (7)$$

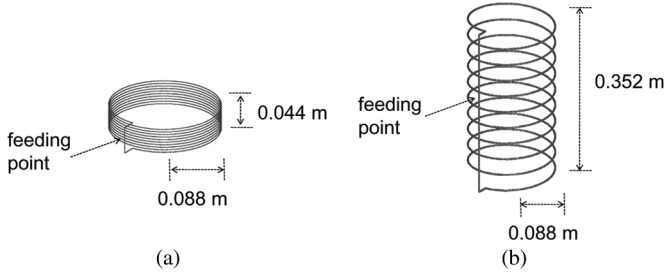


Fig. 3. Two coupled solenoidal small antennas: (a) wide solenoidal small loop, (b) narrow solenoidal small loop

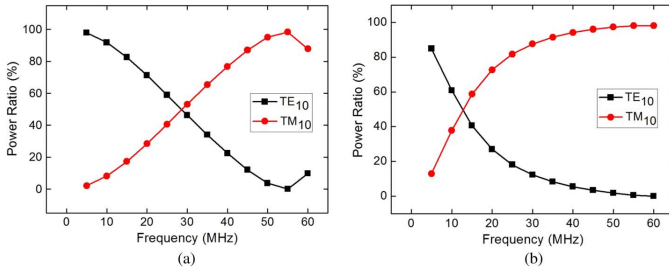


Fig. 4. The power ratio between the TE₁₀ and TM₁₀ modes: (a) wide solenoidal small loop, (b) narrow solenoidal small loop.

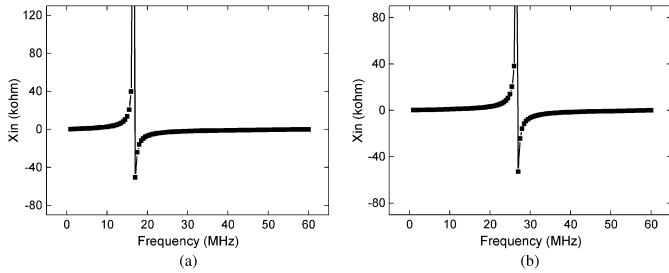


Fig. 5. Reactance of the single solenoidal antenna made of copper wire: (a) wide solenoidal small loop, (b) narrow solenoidal small loop.

respectively, as shown in Fig. 3. By using EM simulation, the power ratios of the TE₁₀ and the TM₁₀ modes in each case are evaluated, as shown in Fig. 4. In both cases, the TE₁₀ mode is the dominant mode at low frequencies, and then the TM₁₀ mode becomes dominant as the operating frequency is increased.

Based on the dominant modes in each case, the operating frequency is set at 11.5 MHz in the wide solenoidal antenna and 20 MHz in the narrow solenoidal antenna. In the former, the TE₁₀ is dominant, whereas the TM₁₀ mode is dominant in the latter.

B. Correction Factor

In [5], the small solenoidal antenna is simply approximated as the combination of the resistor and the inductor, as shown in Fig. 2. Hence, when the antenna is tuned using a series capacitor, the impedance variation of the antenna can be described using a simple RLC series network.

However, the reactance of the solenoidal antenna cannot be simply approximated by a single inductor. According to the reactance characteristics shown in Fig. 5, the solenoidal antenna can be approximated by the parallel LC. The equivalent circuit of the solenoidal antenna is shown in Fig. 6(a), with the self-resonant frequency defined as:

$$\omega_p = (L_{\text{int}} C_{\text{int}})^{-0.5}. \quad (11)$$

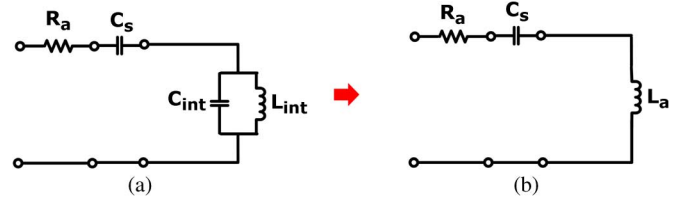


Fig. 6. Equivalent circuit representation of solenoidal antenna: (a) using parallel resonator, (b) using a simplified single element.

If the parallel LC circuit is approximated to a single inductive element, as shown in Fig. 6(b), the equivalent inductor is given as:

$$L_a(\omega) = \frac{L_{\text{int}}}{1 - \omega^2 L_{\text{int}} C_{\text{int}}} = \frac{L_{\text{int}}}{1 - (\omega/\omega_p)^2} \quad (12)$$

and the derivative of the reactance is given as:

$$\frac{d}{d\omega} |\omega L_a(\omega)| = \frac{L_{\text{int}} + \omega^2 L_{\text{int}}^2 C_{\text{int}}}{(1 - \omega^2 L_{\text{int}} C_{\text{int}})^2}. \quad (13)$$

Hence, when the solenoidal antenna is tuned with the series capacitor at the resonant frequency ω_s , the input impedance of the single antenna around the resonant frequency is given by:

$$\begin{aligned} Z_a(\omega_s + \Delta\omega) &\approx j\omega_s L_a(\omega_s) + j\Delta\omega \left(\frac{d}{d\omega} |\omega L_a(\omega)| \right)_{\omega=\omega_s} \\ &+ \frac{1 - \frac{\Delta\omega}{\omega_s}}{j\omega_s C_s} + R_a \\ &= j\omega_s L_a(\omega_s) \left(\frac{2\Delta\omega}{\omega_s} \right) \frac{1}{1 - (\omega_s/\omega_p)^2} + R_a. \end{aligned} \quad (14)$$

From (14), it can be shown that the correction factor defined as

$$1 - (\omega_s/\omega_p)^2 \quad (15)$$

has to be considered to simplify the series-tuned solenoidal loop as a conventional series RLC resonant circuit. Therefore, the 3 dB fractional bandwidth, which is evaluated by (10), also needs to be corrected using the correction factor defined in (15).

C. Comparison

The values of the 3 dB fractional bandwidth, which are calculated by the full EM simulation carried out by the commercial EM software, FEKO, and the proposed method, with consideration of the correction factors, are compared in Table II. In common with [10], the configurations of coupled antennas are classified into four cases according to the relative position and orientation of the antennas, as shown in Fig. 7.

Based on the results of comparison, the estimation of the 3 dB fractional bandwidth using the proposed method with consideration of the correction yields similar results to those based on full EM simulation. The differences between the 3 dB fractional bandwidth evaluated by full EM simulation versus the proposed method are attributed to the deviation in the actual impedance characteristics in the simple model, which uses a single parallel LC resonator.

The results using the method in [5] and the proposed method are compared in Table III. The comparisons are carried out for the parallel configuration that is given in [5]. From the table, it can be seen that the relative errors are improved by using the proposed method.

From the results of Table II, it is clear that the relative error for the diagonal case of the narrow type is relatively large compared to the other cases. This deviation is due to the effect of the higher order modes, which are not considered for the analysis of small antennas [9], [10]. Although the magnitude of the higher order modes (TE_{1,±1} and TM_{1,±1}) is much smaller than the fundamental modes (TE₁₀ and

TABLE II
FRACTIONAL BANDWIDTH OF NEAR-FIELD COUPLED SMALL ANTENNAS

Type (Frequency)	Configuration	Distance	Fractional 3 dB BW ($\Delta\omega_{3dB}/\omega_0$)		
			EM Simulation	Proposed Method Estimated FBW	Relative Error (to the EM Simulation)
Wide (11.5MHz)	Parallel	0.5m	3.48×10^{-3}	3.56×10^{-3}	0.02
		0.7m	2.43×10^{-3}	2.43×10^{-3}	0.02
	Diagonal	0.5m	2.61×10^{-3}	2.66×10^{-3}	0.02
		0.7m	2.26×10^{-3}	2.29×10^{-3}	0.01
	Collinear	0.5m	5.39×10^{-3}	5.93×10^{-3}	0.10
		0.7m	2.78×10^{-3}	2.98×10^{-3}	0.07
	$\pi/4$ -tilted collinear	0.5m	4.17×10^{-3}	4.47×10^{-3}	0.07
		0.7m	2.78×10^{-3}	2.63×10^{-3}	-0.05
Narrow (20MHz)	Parallel	0.5m	18.5×10^{-3}	21.02×10^{-3}	0.14
		0.7m	8.00×10^{-3}	8.50×10^{-3}	0.06
	Diagonal	0.5m	9.00×10^{-3}	11.6×10^{-3} (9.39×10^{-3})*	0.29 (0.04)*
		0.7m	5.50×10^{-3}	5.81×10^{-3}	0.06
	Collinear	0.5m	53.0×10^{-3}	45.61×10^{-3}	-0.14
		0.7m	18.0×10^{-3}	16.99×10^{-3}	-0.06
	$\pi/4$ -tilted collinear	0.5m	27.5×10^{-3}	31.75×10^{-3}	0.15
		0.7m	12.5×10^{-3}	12.52×10^{-3}	0.02

(* means the results with the consideration of the cross coupling of the TE_{10} [or TM_{10}] mode and the $TE_{1,\pm 1}$ [or $TM_{1,\pm 1}$] mode)

TABLE III
FRACTIONAL BANDWIDTH OF NEAR-FIELD COUPLED SMALL ANTENNAS IN PARALLEL CONFIGURATION

Type (Frequency)	Distance	Fractional 3-dB BW ($\Delta\omega_{3dB}/\omega_0$)			
		Proposed Method		Method in [5]	
		Estimated FBW	Relative Error (to the EM Simulation in Table II)	Estimated FBW	Relative Error (to the EM Simulation in Table II)
Wide (11.5MHz)	0.5m	3.56×10^{-3}	0.02	5.34×10^{-3}	0.53
	0.7m	2.43×10^{-3}	0.02	4.32×10^{-3}	0.77
Narrow (20MHz)	0.5m	21.02×10^{-3}	0.14	24.00×10^{-3}	0.29
	0.7m	8.50×10^{-3}	0.06	13.00×10^{-3}	0.63

TABLE IV
SPHERICAL MODES OF THE SOLENOIDAL SMALL LOOP ANTENNAS

Wide Type (at 11.5MHz)		Narrow Type (at 20MHz)	
Modes	Power Ratio	Modes	Power Ratio
TE_{10}	89.32×10^{-2}	TE_{10}	27.01×10^{-2}
TM_{10}	10.52×10^{-2}	TM_{10}	72.70×10^{-2}
$TE_{1,\pm 1}$	0.02×10^{-2}	$TE_{1,\pm 1}$	0.20×10^{-2}
$TM_{1,\pm 1}$	0.16×10^{-2}	$TM_{1,\pm 1}$	0.08×10^{-2}

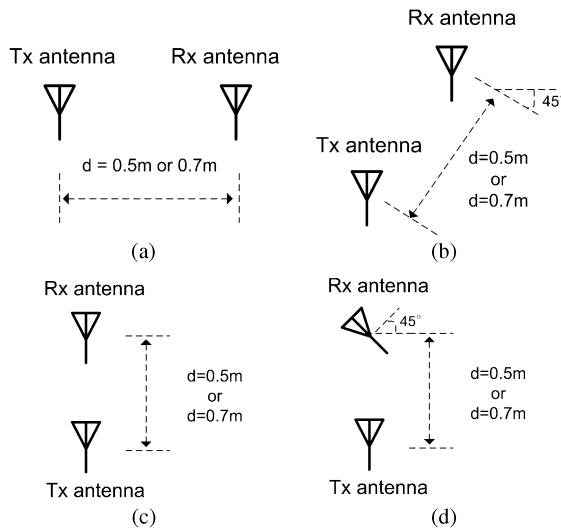


Fig. 7. Configurations of two coupled antennas: (a) parallel configuration, (b) diagonal configuration, (c) collinear configuration, and (d) $\pi/4$ -tilted collinear configuration.

TM_{10}) as shown in Table IV, the cross coupling of the TE_{10} (or TM_{10}) mode and the $TE_{1,\pm 1}$ (or $TM_{1,\pm 1}$) mode can affect the total mutual impedance under the condition that the electrical distance between the coupled antennas is very small. From [9] and [13], the cross coupling can be given as:

$$Z_{12(TE_{1,\pm 1}-TE_{10})} (= Z_{12(TM_{1,\pm 1}-TM_{10})}) \propto \sin(2\theta). \quad (16)$$

Hence, the cross coupling is maximized at the diagonal configuration. Moreover, it can be seen from Table IV that the magnitude of the higher order mode for the narrow solenoid is relatively large compared to the wide solenoid. Hence, the relatively large deviation for the diagonal case of the narrow solenoid can be explained. The calculated results for the diagonal case, including the cross coupling between fundamental and higher order modes, are compared in Table II.

V. CONCLUSION

In this communication, a new method of analysis is proposed for estimating the 3 dB bandwidth of near-field coupled identical small antennas for an NFC system. The proposed analysis is based on the equivalent circuit representation of coupled antennas using a modified coupled resonator circuit. The coupling of the antennas is determined from the mutual impedance evaluated by the addition theorem. Furthermore, a correction factor is proposed that takes into account the intrinsic characteristics of a solenoidal loop antenna. Using the proposed method, the values of 3 dB bandwidth for the near-field coupled wide and narrow solenoidal antennas, where the dominant modes are TE_{10} and TM_{10} , respectively, are investigated. Based on our findings, our proposed analysis yields data that are in good agreement with those of EM simulation.

REFERENCES

- [1] W. L. Stutzman and G. A. Thiele, *Antenna Theory and Design*. New York: Wiley, 1998, ch. 1.
- [2] H. G. Schantz, "Near field propagation law and a novel fundamental limit to antenna gain versus size," in *Proc. IEEE Int. Symp. Antennas Propag.*, Washington, DC, 2005, pp. 237–240.

- [3] E. Strommer, J. Kaartinen, J. Parkka, A. Ylisaukko-oja, and I. Korhonen, "Application of near field communication for health monitoring daily life," in *Proc. IEEE EMBS Annu. Int. Conf.*, New York City, 2006, pp. 3246–3249.
- [4] B. Sklar, *Digital Communication*. Englewood Cliffs, New Jersey: Prentice Hall, 2001, ch. 9.
- [5] H. C. Jing and Y. E. Wang, "Capacity performance of an inductively coupled near field communication system," presented at the IEEE Int. Symp. Antennas Propag., San Diego, CA, 2008.
- [6] G. Shaker, S. Safavi-Naeini, and N. Sangary, "Q-bandwidth relations for the design of coupled multi-element antennas," presented at the IEEE Int. Symp. Antennas Propag., Charleston, SC, 2009.
- [7] Y. Kim and H. Ling, "Investigation of coupled mode behavior of electrically small meander antennas," *Electron. Lett.*, vol. 43, no. 23, 2007.
- [8] Y. Tak, J. Park, and S. Nam, "Equivalent circuit of a two-element spherical small antenna," presented at the IEEE Int. Symp. Antennas Propag., Charleston, SC, 2009.
- [9] J. Lee and S. Nam, "Fundamental aspects of near-field coupling antennas for wireless power transfer," *IEEE Trans. Antennas Propag.*, vol. 58, pp. 3442–3449, 2010.
- [10] Y. Tak, J. Park, and S. Nam, "Mode-based analysis of resonant characteristics for near-field coupled small antennas," *IEEE Antennas Wireless Propag. Lett.*, vol. 8, pp. 1238–1241, 2009.
- [11] W. K. Kahn and W. Wasylkiwskyi, "Coupling, radiation and scattering by antennas," in *Proc. Symp. on Generalized Networks*. Brooklyn, N.Y.: Polytechnic Press, 1966, vol. 16, pp. 83–114.
- [12] H. G. Hong and M. J. Lancaster, *Microstrip Filters for RF/Microwave Applications*. New York: Wiley, 2001, ch. 8.
- [13] W. C. Chew and Y. M. Wang, "Efficient ways to compute the vector addition theorem," *J. Electromagn. Waves Appl.*, vol. 7, no. 5, pp. 651–665, 1993.